Egypt. J. Chem. **Vol. 66**, No. 6, pp. 499 – 510 (2023)

Egyptian Journal of Chemistry

http://ejchem.journals.ekb.eg/

Organic-Inorganic Composites Based on Multi-walled Carbon Nanotubes Containing Lysine/Histidine

Ahmed A. Haroun*, Fathalla A. Ayoob, Ragab A. Masoud

Chemical Industries Research Institute, National Research Centre, 12622 Dokki, Giza, Egypt.

Abstract

Carbon nanotubes (CNTs) have been employed alone or in composites with other substances to generate highly useful materials in a variety of industries. They are especially promising as scaffolds for bone tissue regeneration. To the best of our knowledge, no studies have been published on the usage of lysine (Lys) or histidine (His) for functionalizing oxidised Multiwalled carbon nanotubes (ox-MWCNTs) using the sol-gel process. The goal of this research is to create innovative hybrid composites for biomedical applications based on ox-MWCNTs incorporating tetra ethyl orthosilicate (TEOS) and various amino acids (Lys or His). Fourier transform infrared spectroscopy (FTIR), dynamic light scattering technique (DLS), X-ray diffraction (XRD), thermogravimetric analysis (TGA), scanning and transmission electron microscopes (SEM and TEM) were used to characterise the physicochemical properties.. *In vitro* bone bioactivity was tested after 7 days of soaking in simulated body fluid (SBF) at 37 °C, as well as cytotoxicity against mice bone marrow stromal cells using the MTT assay. The results showed that both functionalized MWCNTs had particle sizes of 1332 and 1329 nm and are colloidal stable. After soaking the composites in SBF, SEM pictures revealed aggregated ca-apatite layers on the surface. After soaking for 7 days, the calcium element and the liberated free amino acids concentrations in the residual SBF were approximately (2.1 and 0.9) and (2.6 and 2.0) mg/L in the case of both amino acids, respectively. It can be concluded that both covalent attached amino acids play enhancement role for the ca-apatite formation and lowering the toxicity in the hybrid composites relative to the ox-MWCNTs especially in the case of His.

Keywords: Multiwalled Carbon nanotubes; lysine; histidine; cytotoxicity; In vitro bone bioactivity; hybrid composites; sol-gel preparation.

1. Introduction

Hybrid composites have attracted increased attention in biomedical sciences and other scientific areas in recent years. One cause for this is the growing demand for regenerative or replacement tissues. It is not unexpected, then, that research into organic-inorganic composites has contributed to the advancement of materials science as a highly interdisciplinary field that employs novel methods to previously exhausted synthesis processes. The utilization of sol-gel technology for biomedical applications is one significant discovery that best exemplifies this point. As a result, this study focuses on developments and prospective applications of research in this sector.

In order to create intelligent nanoscale vehicles, a brand-new multidisciplinary study area called nanobiotechnology combines nanoscience with the biological environment. These vectors may be loaded with more medication and released under the right circumstances [1-5]. With the incorporation of biological substitutes like living cells, biomolecules, biocompatible and biodegradable synthetic materials, or natural materials that can restore, maintain, and improve the function of tissues or organs, tissue engineering aims to restore, repair, and replace damaged and diseased tissues [6-8]. At the moment, therapies for tissue regeneration use isolated cells or cell substrates, the introduction of tissue-induced biomolecules like proteins, medicines, and oligonucleotides, and lastly artificial constructs with or without bio-macromolecules [9, 10]. The designed constructs approach is the most often employed tissue engineering technique. Among these, the development of biocompatible and bioactive biomaterials is vital for tissue engineering. Carbon nanotubes (CNTs) have been widely used in electronic applications, energy storage and photovoltaics, and more recently, medicinal applications due to their outstanding physical features, which include mechanical, thermal, and electrical capabilities. CNTs are often functionalized with different functional groups (such

*Corresponding author e-mail: haroun68_2000@yahoo.com.; (Ahmed A. Haroun).
Receive Date: 22 May 2023, Revise Date: 24 June 2023, Accept Date: 25 June 2023
DOI: 10.21608/EJCHEM.2023.212461.8004

as -OH and -COOH) using covalent and non-covalent methods to increase dispersity in aqueous media and minimize toxicity [11-14]. Nonetheless, the toxicity of carbon nanotubes remains an unsettled question, with various research indicating opposing patterns [15-29]. CNTs have mostly been employed as reinforcement filler in polymer-based scaffolds in the field of tissue engineering, increasing mechanical and electrical properties and permitting the production of scaffolds for neural, cardiac, and bone tissue engineering. Non-toxic, safer, and greener carbon nanotubes and polymeric composites are still predicted, and research into the mechanisms by which CNTs generate toxicity is still needed to better utilize the potential components that cause cytotoxicity and genotoxicity [30]. Histidine is an important amino acid with unique biochemical and physiological properties that plays a variety of roles in all living creatures and acts as a crucial modulator of biomolecule interactions with inorganic substances [31]. Poly (L-histidine) is a pH-responsive polypeptide that, when combined with CNTs, can provide a smart nano-vehicle for intelligent drug delivery [32]. Although effective exfoliation of graphite to graphene has previously been described [33], understanding of their interactions with the sp^2 carbon network is lacking. Much shorter amino acid sequences, on the other hand, can be employed to exfoliate graphite. Previously, cavitational chemistry was used to demonstrate the utilization of a shorter amphiphilic pyren-hexahistidine peptide for one-stage exfoliation and functionalization of carbon nanomaterials [34]. Cell-penetrating peptides (CPPs) are a type of tiny molecule with high membrane permeability that can transport peptides, proteins, and other macromolecules into cells, hence creating a new avenue for exogenous chemicals to enter cells. The inclusion of basic amino acids such as lysine (Lys) and histidine (His) distinguishes the cationic peptide as a type of CPP [35]. Because essential amino acids are positively charged in physiological pH, they can interact non-covalently with negatively charged drug molecules and cell membranes [36]. MTT (3-[4,5-dimethylthiazole-2-yl]-2,5-diphenyltetrazolium bromide) assay is based on the ability of living cells' active mitochondrial dehydrogenase enzyme to cleave the tetrazolium rings of the yellow MTT and form dark blue insoluble formazan crystals that are largely impermeable to cell membranes, resulting in their accumulation within healthy cells. Cell solubilization leads in crystal liberation, which is then solubilized. The amount of live cells is proportional to the concentration of soluble formazan dark blue colour. The degree of MTT decrease was determined by measuring absorbance at 570 nm [37]. Because most research investigations focus on the early stages of cell development *in vitro*, long-term *in vivo* studies, including the degradation of polymeric materials leading to the release of CNTs, must be examined. Current studies look into the low content of CNTs in scaffolds due to fabrication constraints and toxicity, as well as how it trades off scaffold qualities like electrical, mechanical, and biological capabilities. Hence, this work deals with preparation of hybrid composites based on oxidized multi-walled carbon nanotubes (ox-MWCNTs) containing tetraethyl orthosilicate (TEOS) and lysine (Lys) or histidine (His) amino acids using sol-gel technique. The physicochemical characterization by FTIR, DLS, XRD, TGA, SEM and TEM were investigated. *In-vitro* bone bioactivity, after soaking in SBF at 37°C for 7 days, and cytotoxicity against mice bone marrow stromal cells, using MTT assay, were also carried out.

Experimental

2.1 Materials

Multi-walled carbon nanotubes (MWCNTs), carbon content 95%, diameters 6-9 nm×5 μm and tetra ethyl orthosilicate (TEOS) were obtained by Sigma-Aldrich. L(+) lysine (Ly), Mw and L(+) histidine (His), Mw were purchased from Biobasic Canada Inc. and Merck Eurolab, respectively. The cell culture materials were obtained from Cambrex BioScience (Copenhagen, Denmark). All other chemicals and reagents were used as received. The chemical structures were illustrated in Fig 1.

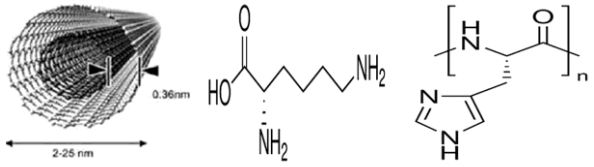

Fig 1. Chemical structures of (a) MWCNTs,(b) L-lysine and (c) L-histidine amino acids.

2.2 Methods

2.2.1. Oxidation and purification of MWCNTs

Olive oil was used to create oxidized MWCNTs (ox-MWCNTs). In a 500 mL flask, 1 g of crude MWCNTs was spread in a mixture of 30% nitric acid and olive oil (3:2 v/v). The flask was then refluxed for 2 h at 110 °C with continuous stirring to produce ox-MWCNTs. The resultant material was filtered under vacuum and extensively washed with 500 mL of chloroform to eliminate any leftover oil [38]. The recovered material was washed with ultrapure water until the filtrate was neutralized (pH 7.0). The obtained substance was vacuum dried for 12 h at 70 °C and stored for later study.

Functionalization of ox-MWCNTs

The sol-gel approach was used to functionalize ox-MWCNTs by hydrolysis and polycondensation of

tetraethyl orthosilicate (TEOS) as a source of SiO_2 with HCl as a catalyst [39] in the presence of various amino acids (Lys or His) as follows: For 1 h, the silicate solutions were agitated with the molar ratios TEOS:C_2H_5OH:H_2O:HCl (1:6:8:0.6). After 2 h, 100 mg of ox-MWCNTs and 100 mg of Lys or His were added and sonicated. Ox-MWCNTs and amino acid moieties were crosslinked in the sol-gel cycle. The sol was poured into plastic moulds and gelled at room temperature for three days. The collected prepared scaffolds have been saved for further research (Table 1).

Table 1 Chemical composition of the prepared scaffolds using sol-gel technique

Sample	Chemical composition (wt/ratio)			
	Ox-MWCNTs	Lys	His	TEOS
(Ox-MWCNTs-TEOS)	1	0	0	1
Scaffold 1	1	1	0	1
Scaffold 2	1	0	1	1

1.2.2. Characterization

The as-prepared scaffolds were characterised using the following analytical tools: Bruker Fourier Transform Infrared Spectroscopy fitted with Attenuated Total Reflectance (FTIR-ATR) was used to explore chemical interactions under the following conditions: scan resolution: 4 cm^{-1}, scan rate: 2 mm/sec, number of scans: 32, range: 400- 4000 cm^{-1}, and mode: transmission. The particle size distribution analysis was performed using dynamic light scattering (DLS) technique by Malvern zetasizer equipment at run time: 2 min, temperature: 25 °C, solvent: water, concentration: 1 mg/mL. The particle forms and morphologies were studied using a Transmission Electron Microscope (TEM) in Tokyo, Japan. Drops of the diluted formulations were placed on a carbon-coated copper grid and allowed to dry at room temperature for 10 minutes before testing. Thermogravimetric analysis (TGA) was used by SETaran- Instrumentation, France, to determine thermal stability. SEM images were captured using the JXA-840A Electron Probe Micro Analyzer JEOL-SEM, Japan, and elemental analysis at the surface was performed using energy dispersive X-ray equipment linked to the SEM. Before being studied with the Polaron SEM Coating Instrument, the substrate was mounted on metal stubs and coated with gold-palladium with a deposit thickness of around 75 at vacuum 710-2 millibar and 2.4 kV cathodic voltage.

The crushed powder sample was subjected to strong X-rays of wavelength 1.54060 A° (CuK) in a 2θ range 4°- 80° at a scan rate of 2°/min and in step size [2°Th.] utilizing PAnalytica Diffractometer System Empyrean, Netherland. The (2θ) values were immediately recorded, and the relative intensities of the diffraction peaks were determined using X-ray diffraction spectra. Agilent 200 series AA Flam Atomic Absorption Spectroscopy was used to determine the calcium element concentration. The liberated free amino acids (Lys and His) in the remaining SBF was investigated using HPLC, after soaking the as-prepared scaffolds for 7 days at 37 °C and pH 7.4, in comparison with the standard amino acids, as previously reported by Zeid AA *et al.* [40]. The HPLC conditions were adjusted as follows: HPLC column: Zorbax Eclipse, detector: diode array, flow rate: 0.75 mL/min, and mobile phases: acetonitrile/methanol (70:30) and (20 mM sodium acetate + 2 mg EDTA + 0.018 mg triethylamine at pH 7.2) in the case of Lys and His, respectively.

1.2.3. *In vitro* bone bioactivity study

In order to replicate the production of apatite on bioactive materials *in vitro*, Kokubo and his colleagues [41] created an acellular simulated body fluid (SBF) with inorganic ion concentrations similar to those of human extracellular fluid. This fluid can be used to assess the bioactivity of artificial materials *in vitro*, as well as to coat apatite on diverse surfaces under biomimetic circumstances. SBF is a metastable solution that contains calcium and phosphate ions that are already supersaturated in relation to apatite. As a result, SBF is prepared as follows: Fill a 1000 mL beaker halfway with ultra-pure water, Stir the water and keep it at 36.5 degrees Celsius. After each reagent has been thoroughly dissolved, add each chemical in the order listed in Table 2. The as-prepared scaffolds were immersed in SBF for 7 days at 37 °C and pH 7.4 before being removed, rinsed with de-ionized water, and dried for further examination. After soaking, the surface of the sample was investigated using SEM and EDX to confirm the production of ca-apatite layers. To guarantee the bioactivity behaviour of the material, the bioactivity test was performed three times [42].

Table 2 Reagents for preparation of SBF (pH 7.25, 1 L).

Order	Reagent	Amount (g)
1	NaCl	7.996
2	$NaHCO_3$	0.350
3	KCl	0.224
4	$K_2HPO_4 \cdot 3H_2O$	0.228
5	$MgCl_2 \cdot 6H_2O$	0.305
6	1 kmol/m^3 HCl	40 cm^3
7	$CaCl_2$	0.278
8	Na_2SO_4	0.071
9	$(CH_2OH)_3CNH_2$	6.057
10	1 kmol/m^3 HCl	Appropriate amount for adjusting pH

1.2.4. *In vitro* cytotoxicity study

Cells and culture

The cytotoxic effect of the examined substances was assessed using mouse bone marrow stromal cells. The RPMI-1640 medium was prepared according to Maridas *et al.* methodology [43], with minor changes. 10% foetal bovine serum (FBS), 2 mM L-glutamine, 100 units/mL penicillin G sodium, 100 units/mL streptomycin sulphate, and 250 ng/ml amphotericin B were added to the medium. At 37 °C, cells were kept sub-confluent in humidified air containing 5% CO_2. When confluence reached 75%, cells were used. Samples were suspended/dissolved in sterile dimethyl sulfoxide (DMSO) and then diluted in media before being added to cells at the desired concentration in the experiment. All experiments were repeated four times. The MTT Cell Viability Assay was used to assess the cytotoxicity of the tested substances against mice bone marrow stromal cells. Cells (0.5X105 cells/90 µl/well) in serum-free media were plated on a flat bottom 96-well microplate and treated for 48 h at 37 °C in a humidified 5% CO_2 atmosphere with 10 µl of different concentrations (200, 100, 50, 25, 12.5 and 6.25, 3.12 µg/mL) of the investigated compounds. Following incubation, the MTT solution was added to the medium at a final concentration of 0.5 mg/mL and incubated for another 4 h. MTT crystals were solubilized by adding (DMSO 90 µl / SDS 60 µl) / well, and the plates were shacked at room temperature before being photometrical determined at 570 nm using a microplate ELISA reader (FLUOstar OPTIMA, BMG LABTECH GmbH, Ortenberg, Germany) [44]. For each concentration, three times were conducted, and the average was obtained. Data were represented as a percentage of relative viability compared to untreated cells compared to the vehicle control, with 100% relative viability indicating cytotoxicity. The percentage of relative viability was calculated as follows:

Absorbance of treated cells/Absorbance of control cells $\frac{\text{Absorbance of treated cells}}{\text{Absorbance of control cells}} \times 100$

Then the half maximal inhibitory concentration (IC_{50}) was calculated from the equation of the dose response curve.

Mode of Cell Death

Cells were dispersed in each well of an 8-well cell culture slide (SPL, Seol, South Korea) so that a volume of 250 µl media contained $1X10^4$ cells and left overnight. The following day, a volume of each sample was added to the labelled wells until the final volume for each sample was 50µg/mL, and the mixture was allowed for another 48 h. After incubation with the materials, the cell sample was stained in a 1:1 ratio with acridine orange/ethidium bromide stain (Sigma Aldrich, Darmstadt, Germany). After 10 min, the slides were photographed using the Zeiss AxioImager Z2 fluorescence microscope (Jenna, Germany).

3. Results and Discussion

3.1. Physicochemical characterization

FTIR-ATR spectroscopy was used to confirm the interaction of ox-MWCNTs with both amino acids (Lys and His). The spectral data are shown in Fig. 2. Unlike ox-MWCNTs, the scaffolds 1 (MWCNTs/TEOS/Lys) and 2 (MWCNTs/TEOS/His) exhibited the expected functional groups. The unique absorption bands emerged at 1640, 1772, and (1533-1605) cm^{-1} in response to C=O, N-H carbonyl stretching, and N-H binding vibrations, respectively. These peaks are clearly the product of interactions between Lys and His groups and ox-MWCNTs. Furthermore, the existence of amide groups at (1303-1374) cm^{-1} shows that amidation interactions may have happened between the carboxyl groups of the ox-MWCNTs and the amino groups of Lys or His. The amino acids (Lys or His) have successfully been linked to the ox-MWCNTs, as seen by the broad bands at (3075-3449) cm^{-1} that correspond to the stretching vibration bonds of O-H groups. The salinized ox-MWCNTs (ox-MWCNTs/TEOS) revealed unique peaks around (2853-2945) and (1415-1433) cm^{-1} during sol-gel synthesis, which were attributed to the stretching and in-plane bending vibrations of the C-H bonds (alkyl groups), respectively. However, the aliphatic sp^3 of ox-MWCNTs is reflected by small peaks at 2920 cm^{-1} [45]. Following sol-gel manufacturing, additional differentiating wear peaks appeared around (1075-1165) and (808-890) cm^{-1}, which correspond to the functional groups Si-O-Si and Si-C (Si-CH_2), respectively. Minor peaks at (663-750) cm^{-1} ascribed to Si-OH groups also emerged, as predicted by the TEOS hydrolysis process [46, 47]. The aforementioned findings, which are consistent with previous work, reveal that both Lys and His amino acids can interact covalently with ox-MWCNTs utilizing the sol-gel approach.

Fig 3 depicts the XRD patterns of the constructed scaffolds 1 (MWCNTs/TEOS/Lys) and 2 (MWCNTs/TEOS/His). Both pure amino acids (Lys and His), which have a high amount of hydrogen bonding, have crystalline structures, as predicted by previous studies [48, 49]. Furthermore, due to its amorphous nature, pure TEOS produced XRD patterns

in the 2θ = 10- 17 range. In the case of ox- MWCNTs, two peaks at 2θ = 25.4 and 42.5 were found as the interlayer spacing d(002) and d(100) reflection peaks, respectively [50]. The scaffolds' phase structure was assumed to be identical to that of the salinized ox-MWCNTs, with the exception that the Lys and His amino acids exhibit unique patterns.

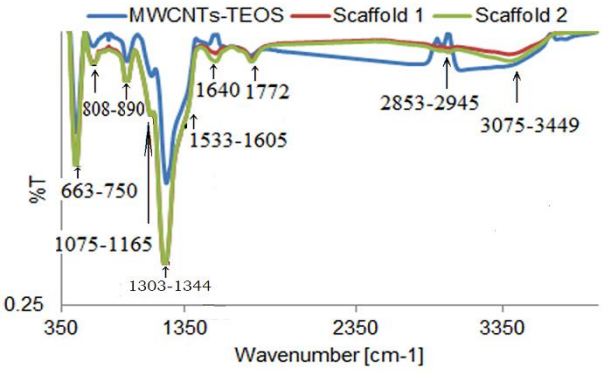

Fig 2. FTIR spectra of the scaffolds 1 (MWCNTs/Lys) and 2 (MWCNTs/His) in comparison with ox-MWCNTs/TEOS.

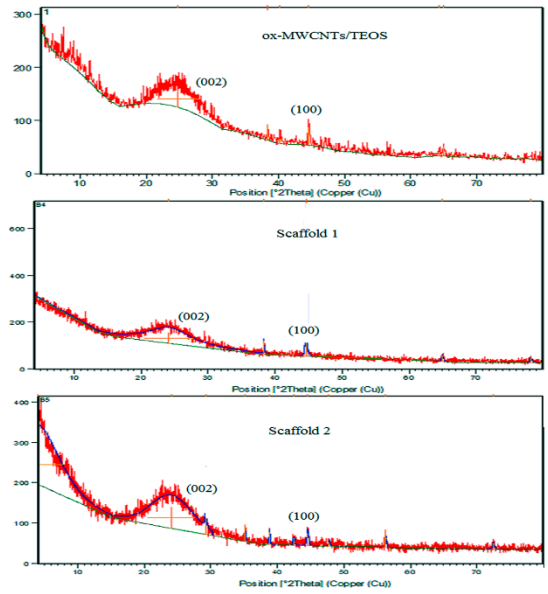

Fig 3. XRD patterns of the scaffolds 1 (MWCNTs/Lys) and 2 (MWCNTs/His) in comparisone with ox-MWCNTs/TEOS.

Table 3 shows the particle size distribution study of the scaffolds as-prepared using the DLS approach. The particle size of salinized ox-MWCNTs grows to 1332 nm and 1329 nm, respectively, with a polydispersity index (PDI) of around 0.62-0.98. The average size of the ox-MWCNTs/TEOS was 413 nm, with a PDI of 0.79. This is most likely attributable to the creation of the core-shell structures. It may also be deduced that the covalent coating of the CNTs network occurred during the interaction of both amino acids with the salinized MWCNTs utilizing the sol-gel process. This is consistent with a previous study of ours that looked at how ox-MWCNTs altered the size of the immobilized enzyme L-asparaginase [51].

Table 3. Particle size measurements of the prepared scaffolds using the DLS technique

Sample	Particle size (d/nm)	Variance (PDI)
(Ox-MWCNTs-TEOS)	413±62	0.79
Scaffold 1	1332±168	0.618
Scaffold 2	1329±25	0.98

Fig. 4 shows TEM images of the scaffolds (c) 1 (MWCNTs/Lys) and (d) 2 (MWCNTs/His) in compared with (a) TEOS and (b) ox-MWCNTs/TEOS. When TEOS was used as a silica precursor, the sol-gel preparation produced spherical particles, as expected. While following the incorporation of amino acids, the aggregation of particles with spherical-like morphology may also be noticed. Both amino acids clearly coated the network of salinized ox-MWCNTs.

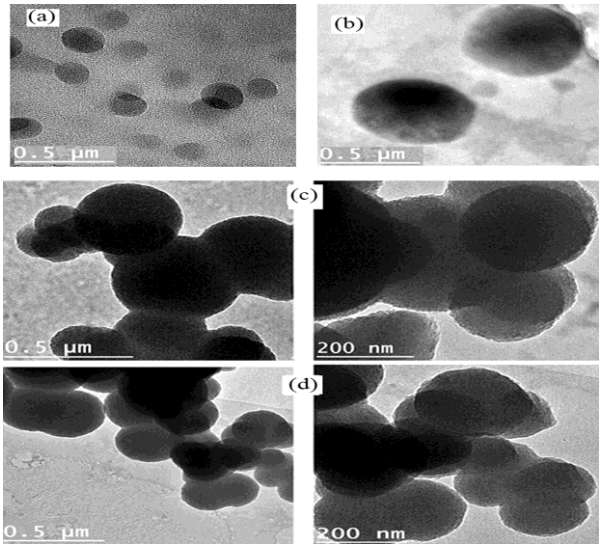

Fig 4. TEM images of the scaffolds 1 (MWCNTs/ Lys, c) and 2 (MWCNTs/ His, d) in comparison with (a) TEOS and (b) ox-MWCNTs/TEOS, at scale bar 500 and 200 nm.

TGA curves for the as-prepared scaffolds are depicted in Fig. 5 (a) for scaffold 1 (MWCNTs/Lys) and (b) for scaffold 2 (MWCNTs/His) in comparison with the pure Lys and His, respectively. Table 4 also includes TGA data (weight loss percentage at various temperatures). In general, all scaffolds (1 and 2) were discovered to have a unique thermal behaviour when compared to pure amino acids. The inclusion of ox-MWCNTs increased the thermal stability of the generated scaffolds 1 and 2 when compared to pure

amino acids, as demonstrated. The weight loss (%) of the generated scaffolds up to 700°C was around 6.64 and 7.57% in scaffolds 1 and 2, respectively, when compared to the pure amino acid samples (1.56%). The marginal increase in thermal stability of the as-prepared scaffold matrices (1 and 2) following the incorporation of ox-MWCNTs can be attributed to the higher thermal conductivity of CNTs, which facilitated heat dissipation within the composites, preventing heat accumulation at certain points for degradation [52].

The liberated free amino acids (Lys and His) in the remaining SBF solution after soaking the scaffolds 1 and 2 for 7 days using HPLC analysis were about 2.6 and 2.0 mg/L, respectively, in comparison with the standards (6.5 and 6.4 mg/L, respectively). This proved that both amino acids were covalently attached with the salinized ox-MWCNTs during sol-gel preparation confirming their high stability in the stored SBF.

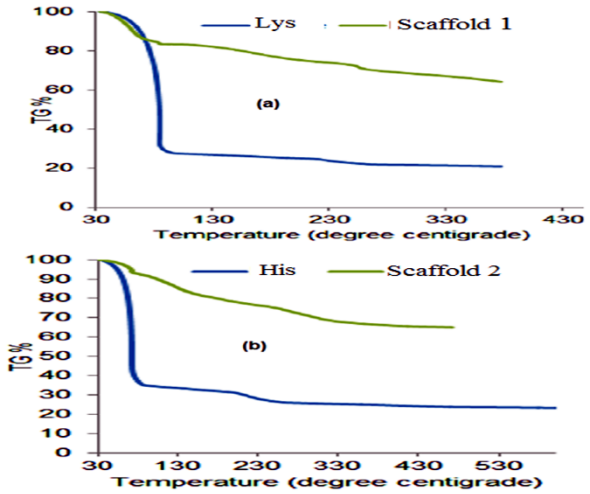

Fig 5. TGA diagrams of the scaffolds 1 (MWCNTs/ Lys) and 2 (MWCNTs/ His) in comparison with the pure amino acids.

Table 4. TGA data of the as-prepared scaffolds at different temperatures in comparison with the Lys and His amino acids.

Sample / temp.	Weight Loss (%) at different temperatures			
	35-100 °C	100–220 °C	220 – 400 °C	400 -700 °C
His	55.5	5.34	4.58	1.56
Lys	72.4	3.56	3.05	----
Scaffold 1	15.46	10.02	11.58	6.64
Scaffold 2	6.78	9.83	10.79	7.57

3.2. In vitro bone bioactivity evaluation

In order to verify the arrangement of the apatite layer on the composite surface, the scaffolds were examined by SEM for a period of 7 days following their withdrawal from the SBF (Figs 6 and 7). The nucleation of apatite may be attributable to the relationship that exists between the surface of composites and the calcium phosphate arrangement. SEM observation at high amplification suggests a close connection between apatite and composites' surfaces, supporting this hypothesis. The particle edifices further associate with $(PO4)^{-3}$ particles due to the supersaturation impacts, framing basic size cores and ensuing development of apatite particles occurs [53]. The interaction between the composites and the SBF solution may produce apatite growth. In other words, the apatite nucleation on the coating after the scaffolds were submerged in SBF for 7 days shows an obvious thick ca-apatite layer aggregation on the whole surface for scaffolds 1 and 2. The apatite layer network is formed into a spherical-like layer, illustrating the effect of the amino acids Lys and His on apatite arrangement enhancement. It was also feasible to witness how apatite, which resembles bone, grew and multiplied on the surface of the composites. SEM images revealed the formation of huge crystal-like formations with microscopic pores crowded together, which aided in the formation of bone. After immersion in SBF, the surfaces of the composites produced assemblies of tiny crystals that looked as island-like highlights. The presence of amino acids clearly increased the amount of apatite islands. The *in vitro* test revealed that the different amino acids (Lys and His) in scaffolds 1 and 2, respectively, demonstrated substantial chemical bioactivity in SBF, whereas the absence of the amino acids in the scaffolds demonstrated weak chemical bioactivity post immersion, as confirmed by SEM. The addition of certain amounts of Lys or His to salinized ox-MWCNTs may be significantly effective, as assessed by their improved bioactivity, according to our findings. Furthermore, the bioactive mechanisms of scaffolds are rapidly improved, with positive effects. When exposed to SBF, an apatite layer resembling bone is claimed to form on the surfaces of the majority of bioactive materials. This calcium phosphate phase resembles the calcium-deficient apatite layer found in living organisms. This process is known as "biomimetic generation of apatite layer producing new materials," and it can provide information about the chemical characteristics of biomaterials [54-56]. Haroun *et al.* [57] discovered a strong relationship between *in vitro* bone-like apatite production from SBF at scaffold surfaces and the various types of amino acids utilized for MWCNTs functionalization. In other words, the uptake of calcium and phosphate from the buffer solution by the

surface of the scaffolds containing distinct amino acids (Lys or His) could trigger bone-like apatite deposition on the surface. As a result, chemical interaction between the surfaces of those composites and bone is expected to occur via apatite in the same way as bioactive materials bond with bone. Using atomic absorption spectroscopy, Fig 8 illustrates the calcium content analysis in the remaining SBF solution after immersing the scaffolds (1 and 2) and the pure amino acids (Lys and His), respectively, relative to the original SBF. The calcium level in the residual SBF was substantially lower for both scaffolds (2.1-0.9 mg/L) as compared to the original SBF (105.3 mg/L). This could be because the scaffolds had both amino acid moieties, which increased Ca absorption from SBF during incubation. Furthermore, the scaffold made according to His amino acid design accelerated the ca-uptake faster than the alternative. This could be due to a decrease in the fluid's supersaturation in relation to the apatite. This result was consistent with previous findings by Miyazaki *et al*.[58].

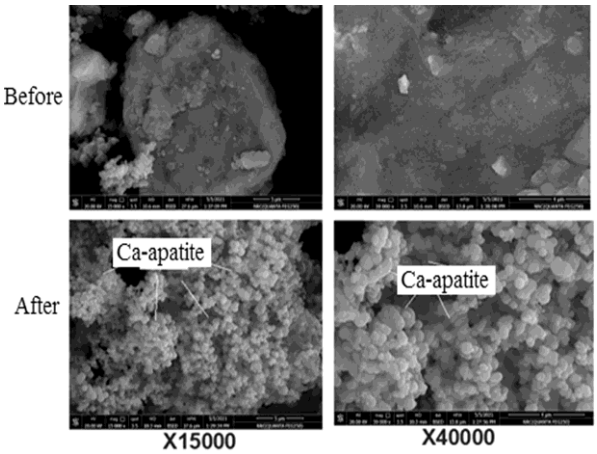

Fig 6. SEM micrographs of the scaffold 1 (MWCNTs/Lys) and before and after soaking in SBF for 7 days at 37ºC (20 Kv and magnifications X15000 and X40000).

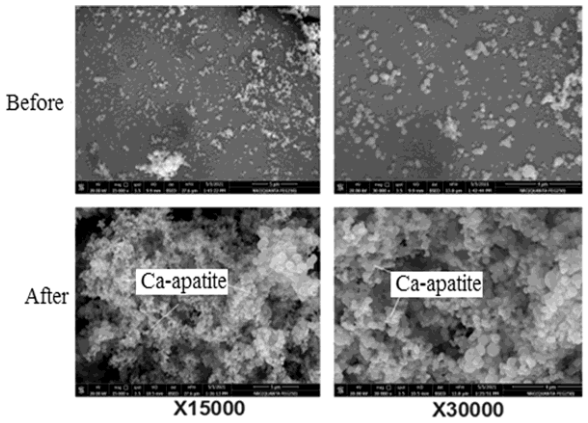

Fig 7. SEM micrographs of scaffold 2 (MWCNTs/His) before and after soaking in SBF for 7 days at 37ºC (20 Kv and magnifications X15000 and X30000).

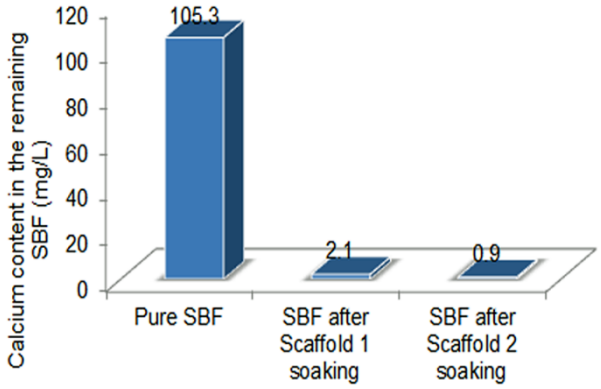

Fig 8. Calcium content determination in the remaining SBF, after soaking the scaffolds 1 (MWCNTs/ Lys) and 2 (MWCNTs/His) for 7 days at 37ºC, in comparison with th the pure amino acids and the original SBF.

3.3. In vitro cytotoxicity evaluation

In this study, we functionalized ox-MWCNTs with two amino acids, Lys and His, and tested their cytotoxicity on a bone marrow stromal cell line. To achieve this goal, we have tracked cell shape, viability, and growth as vital indicators of the cells' physiological state. We chose mice bone marrow cells to investigate the bone toxicity of ox-MWCNTs because they are well characterized cellular models and stable cell lines appropriate for examining nanomaterials' *in vitro* cytotoxic potential. The goal here was to see if these scaffolds were cytotoxic regardless of cell line type or origin. Following a 48-hour exposure to the scaffolds, cell viability, apoptosis, and necrosis were assessed using the MTTA test, and the findings are presented in Fig 9. Cell viability was reduced in cells treated with varied quantities (25, 50, and 100 µg/mL) of as-prepared scaffolds 1 and 2 compared to salinized ox-MWCNTs. Concentrations ranging from 1 to 100 µg/mL often promoted cell viability, as seen by the higher number of viable cells compared to the untreated control. Table 5 shows that after 48 h of incubation, there was a substantial difference in cell proliferation rates between scaffolds 1 and 2 with varied doses. In the case of scaffolds 1 and 2, the viable cell percentages were 45 and 65%, respectively, compared to 90% for the control. It may be inferred that as-prepared scaffold 2 has a beneficial influence on cell proliferation, showing that scaffold containing His has relatively good biocompatibility. Previous research on cellular and molecular mechanisms revealed that the configuration of positively charged essential amino acids improves direct uptake through negatively charged cell membranes *via* non-covalent contact [59]. In other words, the cytotoxicity results of mice bone marrow cells demonstrated that salinized ox-MWCNTs and scaffold 1 including Lys had

significantly more cytotoxic effects on the cells than the control. Their IC_{50} values were 45.39 and 67.92 µg/ml, respectively. At the studied concentrations, the scaffold 2 containing His exhibited practically plateau behaviour. To determine the mode of cell death, mice bone marrow cells were seeded with scaffolds 1 and 2 at concentrations of 50 µg/ml in comparison to salinized ox-MWCNTs for 48 h. The salinized ox-MWCNTs increased cell death *via* necrosis (25%) when compared to the scaffold 1 (necrotic cells reached 15%). Cell apoptosis rates were 10% and 20% in cells treated with Scaffolds 1 and 2, respectively. In contrast, the scaffold 2 did not cause cytotoxicity or cell death, as determined by the method of cell death approach.

Further examination of the overall cell morphology reveals that as-prepared scaffolds at concentrations ranging from 1-100 g/mL did not generate substantial morphological alterations in mouse bone marrow cells, as shown in Fig. 10. The cells had a normal shape, spread and proliferated normally, and formed a monolayer. Our findings contrast with those of Luo *et al.* [60] who found no change in cell shape or loss in cell viability in macrophages treated for 24 h to salinized ox-MWCNTs at concentrations ranging from 0.2 to 200 µg/mL.

Table 5. The percentages (%) of cell viability, apoptosis and necrosis after seeding mice bone marrow cells with the as-prepared scaffolds for 48 h.

Sample	Viable cells	Apoptosis	Necrosis
Control	90%	3%	7%
(Ox-MWCNTs-TEOS)	45%	30%	25%
Scaffold 1	65%	20%	15%
Scaffold 2	80%	7%	13%

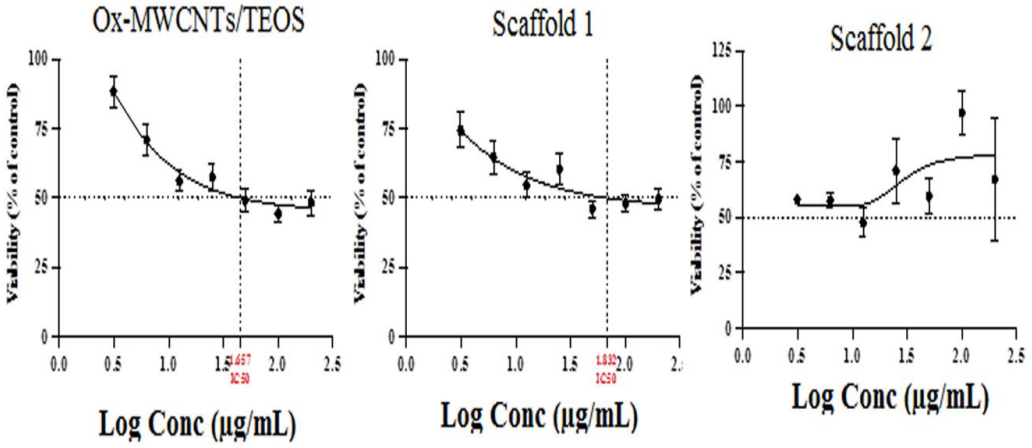

Fig 9. The dose response curve of the scaffolds 1 (MWCNTs/Lys) and 2 (MWCNTs/His) on mice bone marrow cells in comparison with ox-MWCNTs/TEOS using the MTT assay.

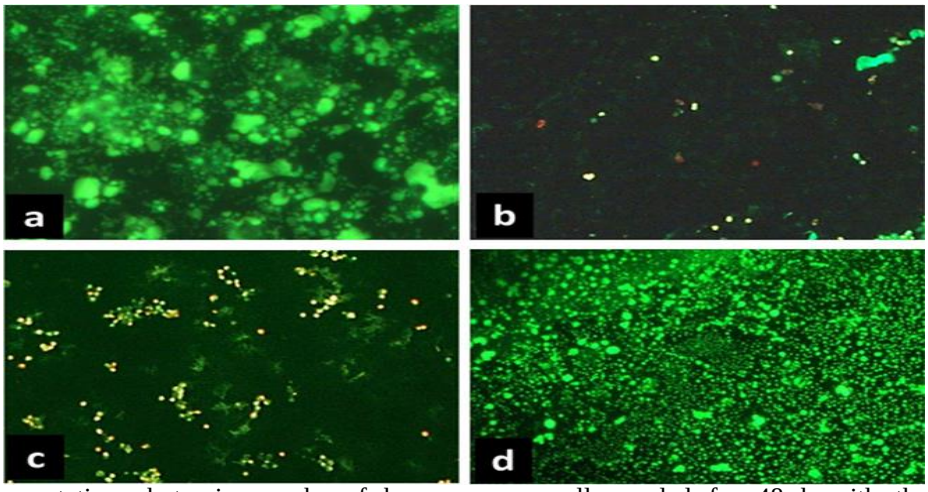

Fig 10. Representative photomicrographs of bone marrow cells seeded for 48 h with the scaffolds 1 (MWCNTs/Lys) (c), and 2 (MWCNTs/His) (d), in comparison with (a) control and (b) ox-MWCNTs/TEOS. The cells were stained with ethidium bromide/ acridine orange dye, magnification power (10X).

Conclusions

The functionalization of ox-MWCNTs with L(+) Lys or His amino acids was accomplished utilizing the sol-gel approach. After soaking in SBF for 7 days at 37 °C, it was revealed that the different amino acids can increase bone-bonding ability. The results of FTIR-ATR, XRD, TGA, TEM, and particle size distribution analyses are useful in understanding the physicochemical properties of the scaffolds developed. Using atomic absorption and HPLC analysis, the calcium content and liberated free amino acids in the remaining SBF were also demonstrated the creation of the apatite layer at the surface of the immersed scaffolds and the covalently bonded amino acids to the ox-MWCNTs. In general, regardless of the amino acid utilized to modify ox-MWCNTs (Lys or His), functionalized ox-MWCNTs were found to have a favourable influence on the viability and proliferation of mice bone marrow cells. In comparison to Lys, His showed a minimal cytotoxic effect. As a result, it is possible to conclude that the functionalized ox-MWCNTs produced by the sol-gel.

Formatting of funding sources

The Egyptian Academy of Scientific Research & Technology, Cairo, Egypt (ASRT).

Acknowledgments

The authors wish to thank The Egyptian Academy of Scientific Research & Technology, Cairo, Egypt (ASRT) for financial supporting of this work according to the Bilateral Joint Project Funding with the Bulgarian Academy of Sciences, Sofia, Bulgaria (BAS) 2020/2023.

References

[1] Wibowo, Y.G., Ramadan, B.S., Taher, T. *et al*. Advancements of Nanotechnology and Nanomaterials in Environmental and Human Protection for Combatting the COVID-19 During and Post-pandemic Era: A Comprehensive Scientific Review. *Biomedical Materials & Devices* (2023). https://doi.org/10.1007/s44174-023-00086-9.

[2] Shahcheraghi, N., Golchin, H., Sadri, Z. *et al*. Nano-biotechnology, an applicable approach for sustainable future. *3 Biotech* 12, (2022) 65. https://doi.org/10.1007/s13205-021-03108-9.

[3] Salem SS. A mini review on green nanotechnology and its development in biological effects. *Arch Microbiol*. 205 (2023) 128. doi: 10.1007/s00203-023-03467-2.

[4] Haleem A., Javaid M., Singh R.P., Rab S., Suman R. Applications of nanotechnology in medical field: a brief review, *Global Health Journal*, 7 (2023) 70-77, https://doi.org/10.1016/j.glohj.2023.02.008.

[5] Rajput A., Shevalkar G., Pardeshi K., Pingale P., Computational nanoscience and technology. *OpenNano,* 12 (2023) 100147, https://doi.org/10.1016/j.onano.2023.100147.

[6] Qinqin X., Lan X., Lin H., Xi Q., Wang M., Quan X. et al. Tumor microenvironment-regulating nanomedicine design to fight multi-drug resistant tumors. *Wiley Interdisciplinary Reviews: Nanomedicine and Nanobiotechnology* 15 (2023) e1842.Doi: 10.1002/wnan.1842

[7] Huang B. Carbon nanotubes and their polymeric composites: the applications in tissue engineering *Biomanufacturing Rev.* 5 (2020) 3. Doi.org/10.1007/s40898-020-00009-x

[8] Harrison BS, Atala A Carbon nanotube applications for tissue engineering. *Biomaterials* 28 (2007)344–353. Doi.org/10.1016/j.biomaterials.2006.07.044.

[9] Sroor F. M, Basyouni W. M, Aly H. F, Younis E. A, Mahrous K..F, Haroun AA. Biochemical and histopathological studies of sulfonylurea derivative as a new chemotherapeutic agent against liver cancer in free- and nano-coated forms. *Appl Biol Chem* **65** (2022) 68. Doi.org/10.1186/s13765-022-00737-3

[10] Pati F, Gantelius J, Svahn HA 3D bioprinting of tissue/ organ models. *Angew Chem Int Ed* 55 (2016) 4650–4665. doi.org/10.1002/anie.201505062

[11] Brtolo P, Chua C, Almeida H, Chou S, Lim A Biomanufacturing for tissue engineering: present and future trends. *Virtual Phys Prototyp* 4 (2009) 203–216. DOI:10.1080/17452750903476288

[12] Lakhdar Sidi Salah, Nassira Ouslimani, Dalila Bousba, Isabelle Huynen, Yann Danlée, Hammouche Aksas. Carbon Nanotubes (CNTs) from Synthesis to Functionalized (CNTs) Using Conventional and New Chemical Approaches. *J. Nanomaterials* (2021) Article ID 4972770, 31 pages. Doi.org/10.1155/2021/4972770.

[13] Aleksandra Benko, Joanna Duch, Marta Gajewska, Mateusz Marzec, Andrzej Bernasik, Marek Nocuń, Witold Piskorz, Andrzej Kotarba.. Covalently bonded surface functional groups on carbon nanotubes: from molecular modeling to practical applications. *Nanoscale* 13 (2021) 10152–10166. DOI: 10.1039/d0nr09057c.

[14] Andreas Breitwieser Uwe B. Sleytr, Dietmar Pum.. A New Method for Dispersing Pristine Carbon Nanotubes Using Regularly Arranged S-Layer Proteins. *Nanomaterials* 11 (2021) 1346. https://doi.org/10.3390/nano11051346.

[15] Boubaker Zaidi, Nejmeddine Smida, Mohammed G. Althobaiti,, Atheer G. Aldajani, Saif D. Almdhaibri.. Polymer/Carbon Nanotube Based Nanocomposites for Photovoltaic Application:

Functionalization, Structural, and Optical Properties. *Polymers* 14 (2022) 1093. Doi.org/10.3390/polym14061093.

[16] Haroun A.A., Taie H.A. Preparation and rational biological evaluation of functionalized carbon nanotube with plant extracts. Proceeding at 2nd Int. Symposium on Materials and Sustainable Development, 9-10 November, Algeria, (2015). DOI: 10.21608/ejchem.2019.16915.2031

[17] Ayoob F.,. Haroun A.A, Nashy E., Mohamed O., Abdelshafy S., Rabi A. Preparation, characterization and in vitro toxicity study of antiparasitic drugs loaded onto functionalized MWCNTs. *Egy J. Chem* 63 (2020) 3829-3836. DOI.10.21608/EJCHEM.2020.23350.2386

[18] Haroun A.A, Ayoob F., Nashy E., Mohamed O., Rabi A. Sol-gel preparation and in vitro kinetic release study of albendazole-immobilized MWCNTs. *Egy J. Chem* 63 (2019) 645-654. DOI: 10.21608/EJCHEM.2019.16915.2031

[19] Haroun A.A, Zaki B.M., Shalash M., Morsy R.A.. Preparation and histological study of multiwalled cacrbon nanotubes bone graft in management of class II furcation defects in dogs. *Open Access Macedonian J Med. Sci.* 7 (2018) 3634-3641. Doi: 10.3889/oamjms.2019.738

[20] Haroun AA, Ahmed H.M, Ahmed E.F. Functionalized multi-walled carbon nanotubes as emerging carrier for biological applications. Proceedings of the 5th World Congress on New Technologies (NewTech'19) Lisbon, Portugal, August 18-20, Paper No. ICNFA 106 (2019)

[21] Haroun A.A,. Amin H.A, Abd El-Alim S.H. Preparation, Characterization and In vitro biological activity of soyasapogenol B loaded onto functionalized multi-walled carbon nanotubes. *Curr Bio Comp* 14 (2018) 364-372. DOI:10.2174/1573407213666170407165917

[22] Haroun A.A,. Amin H.A,. Abd El-Alim S.H. Immobilization and *in vitro* evaluation of soyasapogenol B onto functionalized multi-walled carbon nanotubes. *IRBM* 39 (2018) 35-42. Doi.org/10.1016/j.irbm.2017.12.003

[23] Amin H.A.,. Haroun A.A. Comparative studies of free and immobilized Aspergillus flavus onto functionalized multiwalled carbon nanotubes for soyasapogenol B production. *Egy Pharm J.* 16 (2017) 138-143. **DOI:** 10.4103/epj.epj_28_17.

[24] Haroun A.A., Elnahrawy A.M.,. Abd-Alla H.I. Sol-gel preparation and *in vitro* cytotoxic activity of nanohybrid structures based on multi-walled carbon nanotubes and silicate. *Inorg Nano-Metal Chem* 47 (2017) 1023-1027. Doi.org/10.1080/24701556.2017.1284087

[25] Haroun A.A,. Taie H.A. Cytotoxicity and antioxidant activity of beta vulgaris extract released from grafted carbon nanotubes based nanocomposites. *Macromol. Symp* 337 (2014) 25-33. Doi.org/10.1002/masy.201450303

[26] Haroun A.A., Masoud RA. Preparation and characterization of oxidized multi-walled carbon nanotubes immobilized Aspergillus sp. laccase hybrid materials. *Int. Res. J Multidisciplinary Techno.* 3 (2021) 83-92. Doi.org/10.34256/irjmt21410

[27] Haroun A.A. Carbon nanotubes as innovative materials for bone grafting applications. *Mod Appro Drug Des.* 2 (2019) MADD.000547.2019.

[28] Haroun A.A., Ahmed E.F., Esawy M. Immobilization and characterization of levansucrase enzyme onto functionalized multi-walled carbon nanotubes. *Egypt J Chem* 61 (2018) 667-678. Doi.org/10.21608/EJCHEM.2018.3583.1299

[29] Haroun A.A., Mossa A.H., Mohafrash S.M. Preparation and biochemical evaluation of functionalized multi-walled carbon nanotubes with P. granatum extract. *Curr Bio Comp* 15, (2019) 138-144. DOI: 10.2174/1573407214666180530095912

[30] Costa PM, Bourgognon M, Wang JT, Al-Jamal KT. Functionalised carbon nanotubes: from intracellular uptake and cellrelated toxicity to systemic brain delivery. *J Control Release* 241 (2016).200–219. Doi.org/10.1016/j.jconrel.2016.09.033.

[31] Chen Y., Tao K., Ji W., Kumar V.B., Rencus-Lazar S., Gazit E. Histidine as akey modulator of molecular self-assembly: peptide-based supramolecular materials inspired by biological systems. *Mater. Today* 60 (2022) 106-127. Doi.org/10.1016/j.mattod.2022.08.011

[32] Haghi A., Raissi H., Hashemzadeh H., Farzad F. Development of the poly(L-hitidine) grafted carbon nanotube as a possible smart drug delivery vehicle. *Computers in Biol. Med.* 143 (2022) 105336. Doi.org/10.1016/j.compbiomed.2022.105336.

[33] Guan G.J., Zhang S.Y., Liu S.H., Cai Y.Q., Low M., Teng C.P. *et al.* Protein induces layer-by-layer exfoliation of transition metal dichalcogenides. *J. Am. Chem.* Soc. 137 (2015) 6152-6155. DOI:10.1021/jacs.5b02780

[34] Ihiawakrim D., Ersen O., Melin F., Hellwig P., Janowska I., Begin D. *et al.* A single-stage functionalization and exfoliation method for the production of graphene in water: stepwise construction of 2D-nanostructured composites with iron oxide nanoparticles. *Nanoscale* 5 (2013) 9073-9080.

[35] Kim S.W., Kim N.Y., Choi Y.B., Park S.H., Yang J.M., Shin S. RNA interference in vitro and in vivo using an arginine peptride/siRNA complex

system. J. Control. Release 143 (2010) 335-343. DOI: 10.1016/j.jconrel.2010.01.009

[36] Hao M., Zhang L., Chen P. Membrane internalization mechanisms and design strategies of arginine-rich cell penetrating peptides. Int. J. Mol. Sci. 23 (2022) 9038. Doi.org/10.3390/ijms23169038.

[37] Hansen MB, Nielsen SE and Berg K: Re-examination and further development of a precise and rapid dye method for measuring cell growth/cell kill. *J Immunol Methods* 1989, 119, 203. DOI: 10.1016/0022-1759(89)90397-9

[38] Haider DT., Ahmed DS., Mohamed MR., Haider AJ. Modification of functionalized multi-walled carbon nanotubes by olive oil as economic method for bacterial capture and prevention. *Biosci. Biotech Res. Asia* 14 (2017) 1513-1532. doi.org/10.13005/bbra/2599

[39] Haroun AA., Elnahrawy AM., Maincent P. Enoxaparin-immobilized poly(caprolactone)-based nanogels for sustained drug delivery systems. *Pure Appl. Chem.* 2014, 86, 691. Doi.org/10.1515/pac-2013-1110

[40] Zeid A. A. and Saikh Mo. W. Application of carnon nanotubes in extraction and chromatographic analysis : review. *Arabian J. chem.* 12 (2019) 633- . doi.org/10.1016/j.arabjc.2018.05.012

[41] Kokubo T., Takadama H. How useful is SBF in predicting in vivo bone bioactivity?. *J Biomater* 27 (2006)2907. Doi.org/10.1016/j.biomaterials.2006.01.017

[42] Oyane A, H-M Kim, T. Furuya, T. Kokubo, T. Miyazaki and T. Nakamura,. Preparation and assessment of revised simulated body fluid. *J. Biomed. Mater. Res.* 65A (2003) 188. DOI: 10.1002/jbm.a.10482

[43] Maridas, D. E., Rendina-Ruedy, E., Le, P. T., Rosen, C. J. Isolation, Culture, and differentiation of bone marrow stromal cells and osteoclast progenitors from mice. *J visualized experiments* 131 (2018) 56750. DOI: 10.3791/56750

[44] Nga N.T.H., Ngoc T.T.B., Trinh N.T.M., Thuoc T. L., Thao D.T.P. Optimization and application of MTT assay in determining density of suspension cells. *Analytical Biochem* 610 (2020) 113937. DOI: 10.1016/j.ab.2020.113937

[45] Lee H.J., Oh S.J., Choi J.Y., Kim J., Han L.S., Back J.B. In situ synthesis of poly(ethylene terephthalate) (PET) in ethylene glycol containing terephthalic acid and functionalized multiwalled carbon nanotubes (MWNTs) as an approach to MWNT/PET nanocomposites. *Chem. Mater.* 17 (2005) 5057-5064. Doi.org/10.1021/cm051218t

[46] Avilés F., Cauich-Rodríguez J.V., Rodríguez-González J.A., May-Pat A. Oxidation and silanization of MWCNTs for MWCNT/vinyl ester composites. *eXPRESS Polym Lett* 5 (2011) 766-776. Doi.org/10.3144/expresspolymlett.2011.75

[47] Goyanes S., Rubiolo G.R., Salazar A., Jimeno A., Corcuera M.A., Mondragon I. Carboxylation treatment of multiwalled carbon nanotubes monitored by infrared and ultraviolet spectroscopies and scanning probe microscopy. *Diamond Related Mater* 16 (2007) 412-417. doi.org/10.1016/j.diamond.2006.08.021

[48] Gomes E.J., Lima J.A., Freire P.T.C., Pinheiro G.S, de Sousa F.F., Remédios C.M.R., Effect of Fe (III) on L-asparagine monohydrate investigated under low-and high-temperature conditions. *Spectrochimica Acta Part A: Mol Biomol Spectroscopy* 241 (2020) 118643. doi.org/10.1016/j.saa.2020.118643

[49] Courvoisier E., Williams P.A., Lim G.K., Hughes C.E., Harris K.M. The crystal structure of L-arginine. *Chem. Commun*. 48 (2012) 2761-2763. Doi.org/10.1039/C2CC17203H.

[50] Hsu Y.W., Wu C.C, Wu S.M., Su C.C. Synthesis and propertie of carbon nanotube-grafted silica nanoarchitecture-reinforced poly(lactic acid). *Materials* 10 (2017) 829-844. Doi.org/10.3390/ma10070829.

[51] Haroun A.A., Ahmed H. M., Mossa A.H., Mohafrash S.M., Ahmed E.F. Production, characterization and immobilization of *Aspergillus versicolor L-asparaginase* onto multi-walled carbon nanotubes. *Biointer Res. Appl. Chem.* 10 (2020) 5733-740. doi.org/10.33263/BRIAC104.733740.

[52] Huxtable ST, Cahill DG, Shenogin S, Xue L, Ozisik R, Barone P, Usrey M, Strano MS, Siddons G, Shim M, Keblinski P. Interfacial heat flow in carbon nanotube suspensions. *Nat Mater*. 2 (2003) 731-734. Doi.org/10.1038/nmat996.

[53] Zhu P., Masuda Y., Koumoto K. The effect of surface charge on hydroxyapatite nucleation *Biomaterials* 25 (2004) 3915-3921. Doi.org/10.1016/j.biomaterials.2003.10.022

[54] Abdel-Hamid M.S., Saad M.W., Badawy G.A., Hamza H.A., Haroun A.A. Synthesis and examination of hydroxyapatite nanocomposites based on alginate extracted by *Azotobacter chroococcum* new strain MWGH-ShKB in vitro. *Bioscience Res* 1 (2018) 3293-3306.

[55] Haroun A.A., Beherei H.H.,. Abd El-Ghaffar M.A. Preparation, characterization and *in vitro* application of composite films based on gelatin and collagen from natural resources. *J Appl Polym Sci* 116 (2010) 2083-2094. Doi.org/10.1002/app.31714

[56] Haroun A.A., Migonney V. Synthesis and *in vitro* evaluation of gelatin/hydroxyapatite graft copolymers to form bionanocomposites. *Int J Biol Macromol* 46 (2010) 310-316. Doi.org/10.1016/j.ijbiomac.2010.01.005

[57] Haroun A.A., Gospodinova Z., Krestiva N. Amino acid functionalization of multi-walled carbon nanotubes for enhanced apatite formation and biocompatibility. *Nano Biomedicine Eng.* 13 (2021) 380. Doi.org/10.5101/nbe.v13i4.p380-393

[58] Miyazaki T., Imamura M., Ishida E., Ashizuka M., Ohtsuki C. Apatite formation abilities and mechanical properties of hydroxyethylmethacrylate-based organic-inorganic hybrids incorporated with sulfonic groups and calcium ions. *J. Mater. Sci. Mater. Med.* 20 (2009) 157-161. Doi.org/10.1007/s10856-008-3556-5

[59] Guidotti G., Brambilla L., Rossi D. Cell-penetrating peptides: from basic research to clinics. *Trends Pharmacol. Sci*. 38 (2017) 406-424.

[60] Luo M., P. Chen, J. Wang, *et al.* The cytotoxicity of oxidized multi-walled carbon nanotubes on macrophages. *Sci. China Chem.* 59 (2016)918-926. Doi.org/ 10.1016/j.toxrep.2016.01.011